References and Notes

1. J. V. Byrne, *Ore Bin* **24**, 65 (1962).
2. W. A. Rinehart and J. W. Berg, Jr., *J. Geophys. Res.* **68**, 5613 (1963).
3. J. H. Whitcomb, B. H. Erickson, J. W. Berg, Jr., *Abstr. Geol. Soc. Amer. Cordilleran sect.* (1965), p. 58.
4. N. J. Maloney, thesis, Oregon State University, 1965.
5. N. J. Maloney and J. V. Byrne, *Ore Bin* **26**, 77 (1964).
6. G. A. Fowler, *ibid.* **28**, 53 (1966).
7. R. M. Kleinpell, *Miocene Stratigraphy of California* (American Assoc. of Petroleum Geologists, London, 1938).

8. Supported by a grant from the Office of Naval Research, contract Nonr 1286(10). We thank P. Dehlinger, J. McCauley, and S. Borden for reviewing this report.

2 September 1966

Galactic Depolarization of the 21-Centimeter-Wavelength Radiation of Extragalactic Sources

Abstract. *The dependence of the degree of linear polarization of the radiation from 213 extragalactic sources on galactic coordinates was investigated at 21-centimeter wavelength. In addition to the previously known latitude effect, the depolarization of the radiation during transit through our galaxy is also a function of galactic longitude. One possible explanation is that galactic depolarization is a simple function of the distance traveled by the radiation through an extended galactic halo.*

Observations at wavelengths near 21 cm have shown that the radiation from extragalactic sources located in directions of low galactic latitude is measurably depolarized during its passage through our galaxy (*1, 2*). In addition, internal depolarization is believed to take place in the sources themselves. The galactic depolarization may be caused by differential Faraday rotation across the angular extent of the source as a result of differences in the interstellar magnetic field, or electron density, or both, occurring over distances of the order of 1 parsec or less (*1*).

Polarization results are now available for a larger sample of extragalactic sources, and our results indicate that the depolarization is a function of galactic longitude as well as latitude, with the amount of depolarization tending to increase as the direction to a source approaches the direction of the galactic center.

During August and September 1964, we measured the effective linear polarizations of 76 additional sources at 21.2-cm wavelength with the 300-foot (91.4-m) transit radio telescope of the National Radio Astronomy Observatory at Green Bank, West Virginia. These observations were a continuation of measurements made with the same telescope and receivers in 1963 (*1*). Two identical receivers were connected to orthogonal, linearly polarized outputs of a circular wave guide feed antenna mounted at the focus of the reflector. The orientations of the planes of polarization accepted by the receivers could be varied by rotating the feed antenna. The equipment and methods of observation have been described in detail (*1*). Both the 1963 and 1964 observations were confined to small-diameter (average < 1′) sources of nonthermal spectra selected primarily from the 3C catalog (*3*). Sources for which the data indicate that polarized foreground radiation from our galaxy may introduce appreciable errors were eliminated, leaving a total of 134 presumably extragalactic sources measured at 21.2-cm wavelength with the 300-foot telescope. The estimated uncertainties in the degrees of polarization average about 1 percent standard error. We have combined our data with the results of other observers to give the linear polarizations of 213 extragalactic sources at 21-cm wavelength, and have analyzed these data for a dependence on galactic longitude as well as latitude. We have included the results from the Owens Valley Radio Observatory as given by Morris and Berge (*4*), and the results of Bolton, Gardner, and Mackey; Gardner and Davies; and Gardner from the Parkes catalog of radio sources (*5, 6*).

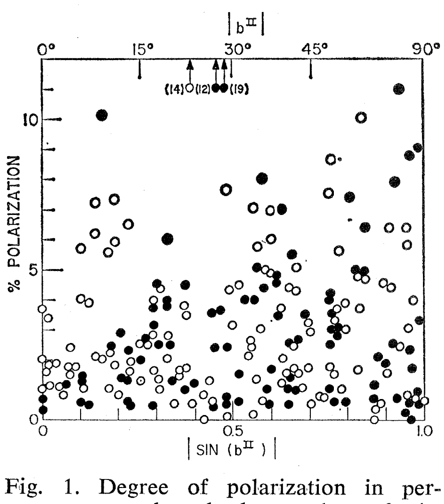

Fig. 1. Degree of polarization in percent versus the absolute value of the sine of the galactic latitude. Open circles represent sources in the galactic longitude range $90° < \ell^{II} \leq 270°$ and solid circles represent sources in the range of $270° < \ell^{II} \leq 360°$ and $0° < \ell^{II} \leq 90°$.

The degrees of linear polarization of the 213 sources are plotted as a function of the absolute value of the sine of the galactic latitude in Fig. 1. The open circles represent sources in the 180° range of galactic longitudes on the galactic anticenter side of Earth, and the solid circles represent sources in the hemisphere centered on the galactic center side of Earth. The sample contains 93 sources on the galactic center side in longitude and 120 sources on the anticenter side. Figure 1 indicates that sources at low latitudes tend to be less strongly polarized than sources at high latitudes; this finding confirms the latitude dependence found previously (*1*). However, the present larger sample shows that the effect is especially pronounced for sources having longitudes on the galactic center side of Earth. Figure 1 shows that almost all the sources of low galactic latitude (less than 15°) that are appreciably polarized are on the galactic anticenter side of Earth, where the distances traveled by the radiation through our galaxy are relatively short. The chi-square test applied to the distribution of polarization versus latitude for the data represented by the open circles in Fig. 1, or applied to the data represented by the solid circles, or applied to all the data combined, gives in each case probabilities of less than 5 percent that the distributions of polarizations are intrinsically the same for high and low latitude sources.

Figure 2 is a plot of degree of polarization versus galactic longitude for each of the 213 sources. The sources of the sample having absolute values of latitude equal to or less than 15° are represented by solid circles, and the sources of absolute latitude greater than 15° are represented by open circles. Figure 2 again illustrates that most low latitude sources in the 180° range of longitudes toward the galactic center are not appreciably polarized, while about one-third of the low latitude sources on the anticenter side show appreciable polarization. The chi-square test gives a probability of about 6 percent that the apparent difference in the polarization distributions for the low latitude sources is due to random sampling.

One possible interpretation of the data is that the depolarization is a direct function of the length of the path traveled by the radiation through the galaxy. In this case, if the depolariza-

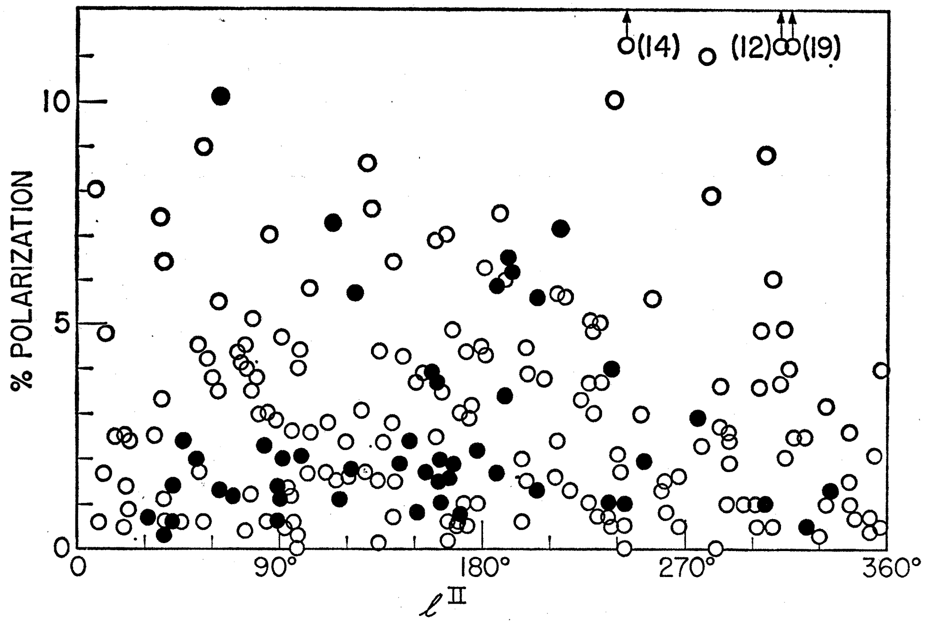

Fig. 2. Degree of polarization in percent versus the galactic longitude. The solid circles represent sources that are within 15° of the galactic plane in latitude, and the open circles represent sources that are more than 15° from the plane.

tion took place in a very thin layer parallel to the galactic plane, we would expect the depolarization to be a function of latitude only, unless the outer boundary of the layer is just slightly farther than Earth from the galactic center, as has been found by Westerhout (*7*) for the distribution of detectable ionized hydrogen. Spitzer (*8*) has proposed a possible galactic corona of rarified, high-temperature gas. For a coronal temperature of 500,000°K the ionized gas will extend to a height of 5000 parsecs above the galactic plane (*8*).

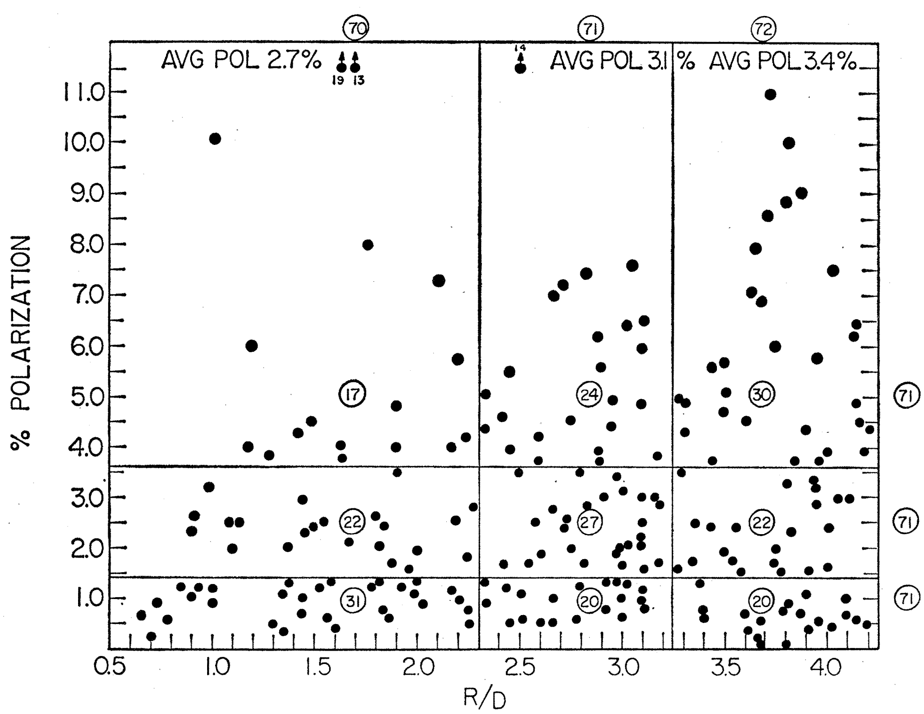

Fig. 3. Degree of polarization in percent versus the ratio of R to D, where D is the path length in the direction of the source from Earth to the outer boundary of an oblate-spheroid model galaxy formed by rotating an ellipse about its minor axis, for a semiminor axis of 5000 parsecs, a semimajor axis, R, of 15,000 parsecs, and for Earth located in the galactic plane at a distance of 10,000 parsecs from the center. The circled numbers give the populations of the rows, columns, and rectangles, and these are the populations that were used in the chi-square test.

Figure 3 is a plot of the degrees of polarization versus the ratios of the semimajor axis, R, to the path lengths, D, through a corona of this extent. We have represented the corona by an oblate spheroid having a semiminor axis, Z, of 5000 parsecs and a semimajor axis, R, of 15,000 parsecs, with Earth situated in the central plane 10,000 parsecs from the center. Figure 3 shows that sources for which the path lengths, D, in this model are long tend to be less strongly polarized than sources for which the path lengths are relatively short. The chi-square test gives a probability of only 3 percent that the distributions of polarization for sources of short and long path lengths in this model are intrinsically the same. It is probable that the explanation of galactic depolarization is not as simple as that suggested by the model used for Fig. 3, and other, very different models may also be consistent with the data. However, the fact that this simple model serves to relate degree of polarization and galactic coordinates gives strong evidence that galactic depolarization is a function of galactic longitude as well as latitude.

It can be shown (*1*) that galactic depolarization at 21 cm can be explained by variations in the interstellar magnetic field or by electron density, or both, with scales of the order of 1 parsec or less. The available polarization data appear to be consistent with a component of interstellar magnetic field with small-scale reversals of direction, or effectively closed loops, superimposed on a fairly uniform field. The average total Faraday rotation at 21-cm wavelength is only of the order of 4 radians at low latitudes and varies slowly with galactic coordinates (*9*), while depolarization requires differential Faraday rotations of roughly 2 or 3 radians over the very small angular diameters of most of the sources.

J. M. Bologna
E. F. McClain
R. M. Sloanaker

E. O. Hulbert Center for Space Research, Naval Research Laboratory, Washington, D.C. 20390

References and Notes

1. J. M. Bologna, E. F. McClain, W. K. Rose, R. M. Sloanaker, *Astrophys. J.* **142**, 106 (1965).
2. P. Maltby, *ibid.*, p. 621. ———, *ibid.* **144**, 219 (1966).
3. D. O. Edge, J. R. Shakeshaft, W. B. Mc-

Adam, J. E. Baldwin, S. Archer, *Mem. Roy. Astron. Soc.* **68**, 37 (1959); A. S. Bennett, *ibid.*, p. 163.
4. D. Morris and G. L. Berge, *Astron. J.* **69**, 641 (1964).
5. J. G. Bolton, F. F. Gardner, M. B. Mackey, *Australian J. Phys.* **17**, 340 (1964); R. M. Price and D. K. Milne, *ibid.* **18**, 329 (1965); G. A. Day, A. J. Shimmins, R. D. Ekers, D. J. Cole, *ibid.* **19**, 35 (1966).
6. Since completion of the analysis necessary for the present paper, Gardner and Davies [*Australian J. Phys.* **19**, 441 (1966)] have published polarization measurements which include the results for an additional 46 sources. While these additional data are not included in the present report, preliminary analysis indicates that these data will not alter our conclusions.
7. G. Westerhout, *Bull. Astron. Inst. Neth.* **14**, 215 (1958).
8. L. Spitzer, Jr., *Astrophys. J.* **124**, 20 (1956).
9. D. Morris and G. L. Berge, *ibid.* **139**, 1388 (1964); F. F. Gardner and R. D. Davies, *Australian J. Phys.* **19**, 129 (1966).

23 September 1966

Crystal Structure of Amylose Triacetate: A Nonintegral Helix

Abstract. *The x-ray diffraction diagram of an oriented fiber of amylose triacetate I, presenting evidence for a nonintegral helical structure, was analyzed by a model and by Fourier transform calculation. The results suggest a helical structure with 4.67 ± 0.02 residues per one turn of the helix, which appears to be left-handed.*

In studying x-ray diffraction diagram of amylose triacetate, whose crystalline form was first observed by Whistler and Schieltz (*1*), we noted evidence of helical conformation of the polymer chain. As fiber diagrams usually contain a minimum of information regarding the structure of the polymer, this indication presented an attractive starting point for an attempt to solve the crystal structure of amylose triacetate.

Amylose, the linear polymer of α-1, 4-D-glucose which occurs in starch, is easily acetylated by means of a nondegradative procedure (*2*). The triacetate can be cast into a film from chloroform solution. The film is partly crystalline and may be oriented by stretching in glycerol at 160°C to an extension of at least 500 percent (*1*). An x-ray diffraction diagram of this structure, termed amylose triacetate I, taken with CuKα radiation on flat film with the x-ray beam perpendicular to the surface of the film (Fig. 1), indicates a high degree of parallel orientation of the crystallites and shows the typical features of scattering from a helical structure: an x-shaped distribution of intensities about the center of the diagram and a single strong reflection on the equator, suggestive of hexagonal close packing. Some degree of translational disorder in the structure is indicated by streaking of reflections on layer lines other than the equator. The lack of streaking on the equator shows the absence of variation in the lateral distance between the chains.

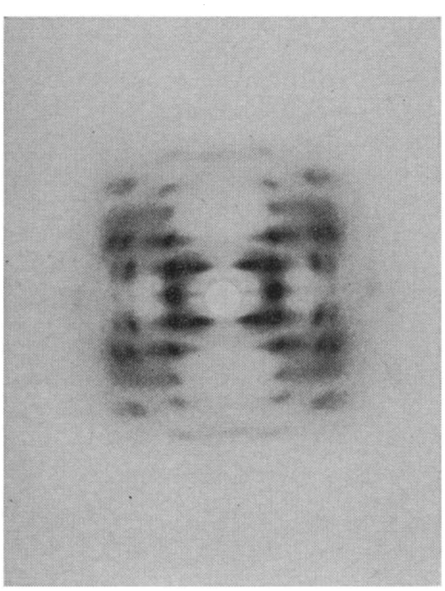

Fig. 1. X-ray diffraction diagram (flat film) of an oriented film sample of amylose triacetate I. CuKα radiation; flat-film vacuum camera; film-to-sample distance, 5 cm; x-ray beam perpendicular to surface of sample; and fiber axis vertical.

Quantitative appraisal of this diagram, as well as of others taken with the sample inclined with respect to the primary x-ray beam, showed the following: (i) the packing of chains is indeed hexagonal, with the lateral distance between chains 10.87 Å; (ii) although all reflections fall on clearly resolved layer lines, the separation of layers in reciprocal space is not constant and cannot be accounted for with a single fiber repeat (Fig. 2A); (iii) there is only one meridional reflection present. These data indicate that the amylose triacetate chain is helical and that the helix is nonintegral; that is, within one turn of the helix there is no structural repeat. The advance (axial thrust) per turn is 17.6 ± 0.2 Å, as obtained from the first-layer line spacing, and the advance per residue is 3.64 ± 0.06 Å, as obtained from the meridional reflection. The ratio 17.6/3.64 indicates that the number of residues per turn of the helix is in the vicinity of 4.8 to 4.9.

Scale models of such a helix were constructed for both the left-handed (*3*) and the right-handed case (the handedness of the helix could not be determined from the x-ray diagram), and both conformations proved stereochemically sound, although the left-handed helix seemed more probable on the basis of better cylindrical symmetry and a higher degree of compactness.

The essential agreement between the scale models and the above interpretation of the fiber diagram prompted a more quantitative examination of the proposed structure, as the monomers-per-turn ratio was still approximate and the handedness of the helix could not be determined from the scale models only. This examination took the form of the calculation of Fourier (or molecular) transforms. Since the molecular transform is essentially the diffraction diagram of one molecule, it is of value in a quick comparison of the scattering from an assumed molecular conformation and the observed diffraction diagram. The calculation of molecular transforms for helical structures is relatively easy, as one needs only the cylindrical coordinates of the atoms of one asymmetric unit of the helix (in most instances one monomer residue) and not the relative positions of the atoms with respect to the crystallographic unit cell, as required by the ordinary structure factor calculations. The intensity, I, at any point in the helix transform is given by the following expression (*4*):

$$I \propto F^2 \qquad (1)$$

$$F(R, \psi, \zeta) = \sum_n \sum_j f_j J_n(2\pi r_j R) \times \exp\left[i\{n(\psi - \phi_j + \pi/2) + 2\pi z_j \zeta\}\right] \qquad (2)$$

where $F(R, \psi, \zeta)$ is the Fourier transform at a point in reciprocal space with cylindrical coordinates R, ψ, ζ; r_j, ϕ_j, z_j are the cylindrical coordinates of the jth atom; J_n $(2\pi r_j R)$ is the nth-order Bessel function (whose value is determined by the argument in parentheses); and f_j is the scattering factor for the jth atom.

The calculation of the above transform is facilitated by casting it in the